International Journal of Advanced Science and Technology
Vol. 29, No. 03, (2020), pp. 8332 - 8339

Synthesis and Characterization Hausmannite (Mn_3O_4) Nanoparticle of Manganese Ores Prepared By High-Energy Milling

Ratnawulan[1], Fuji Prasetyo[1], Ahmad Fauzi[1], Ramli[1]

[1]*Physics Department, Universitas Negeri Padang, Padang, Indonesia*

Corresponding author: ratnawulan@fmipa.unp.ac.id

Abstract

In this paper we report synthesis and characterization of hausmanite (Mn3O4) manganese ores nanoparticles from West Sumatera deposit by High- Energy Milling method. The synthesis was carried out using sintering temperature variation of 26 ° C, 600 ° C, 700 ° C, 800 ° C, 900 ° C, and 1000 ° C and milling time of 0 hours, 2 hours, 4 hours, 8 hours and 10 hours. Characterization is done by using X-Ray Fluorescence (XRF) and X-Ray Diffraction (XRD) and Scanning Electron Microscopy (SEM). XRF test results showed that the manganese content was 84.139%. The Hausmanite phase was obtained when the sample was sintered at 700^{0}C. The crystal structure of the Hausmanite phase is tetragonal. We obtained the the hausmanite nanoparticles with homogeneous size distribution could be synthesized at 8 hours of grinding time. The size of the nanoparticles produced is 90.50 nm.

Keywords : *Hausmanite (Mn3O4), nanoparticles, High-Energy*

1. Introduction

Manganese ore processed by certain material engineering techniques will create a new phase that has an economic value of hausmannite (Mn_3O_4). Hausmannite (Mn_3O_4) includes most stable manganese oxide minerals compared to other types of manganese oxides. Hausmannite is brownish brown and shiny as metal and has a high melting point of 1560 ° C [1]. Hausmannite in nanoparticle size is widely used for base coatings on steels that can improve mechanical properties [2] and as corrosion inhibiting pigments [3]. The manufacture of nano-sized materials or particles has the purpose of improving the material properties. The increasing material properties often observed in nano fabrication are surface area, melting point, reactivity, conductivity, and mechanical strength.

The synthesis of nanoparticles means the manufacture of particles of less than 100 nm and at the same time altering their properties or functions. The synthesis of nanoparticles is generally divided into 2 ie top down and bottom up. An example of a top-down method is grinding with a milling tool, while the bottom-up method uses sol gel techniques, chemical precpitation, and phase agglomeration [4]. The grinding method using a ball mill, has several advantages such as this method is very simple, cheap, the product is very small, and can produce homogeneous products using ball mill [5].

Various studies have been done previously on hausmannite nanoparticles, including using the hydrothermal method with EDTA-2Na base material [6]. The synthesis of hausmannite nanoparticles has also been performed using a solvent-free method with basic materials of manganese (II) acetate, trioxadecanoic acid (TODA), and ammonium acetate [7]. In addition, solvothermal methods have also been used to s ynthesize these hausmannite nanoparticles by using Mn $(CH_3COO)_2.4H_2O$ as precursors and oleic acids as surfactants [8].

In general, the method of synthesis of hausmannite nanoparticles that has been done previously using synthetic mineral materials where its limited availability, costly and long

ISSN: 2005-4238 IJAST

time in the manufacture of materials and the need for complex control of reaction conditions. This article contains the synthesis and characterization of hausmannite nanoparticles whose material availability is derived from natural minerals that are materials derived from manganese ore.

2. Experimental

2.1. Sample Preparation:

Manganese ore as a base ingredient Hausmanite taken from the area of West Sumatra. The cleansed manganese ore was crushed using mortar and mortar for 3.5 hours and sieved using an automatic 0.075 mm sieve. Samples were sintered with temperature variations of 26 ° C, 600 ° C, 700 ° C, 800 ° C, 900 ° C, and 1000 ° C to obtain the hausmanite phase. The samples containing the most hausmannite phases were then milled using High Energy Milling Ellipse 3D (HEM-E-3D) with a milling time variation of 0 hours, 2 hours, 4 hours, 8 hours and 10 hours . The ratio of the sample mass to the milling balls is 1:10.

2.2. Characterization

To find out the percentage of manganese ore content composition was measured using X-Ray Fluorescence (XRF) type Epsilon. After the samples were sintered with temperature variations and samples were tested using X-Ray Diffraction (XRD) with the aim of knowing the structure and size of the crystals [9]. The crystal size of Mn_3O_4 hausmannite nanoparticles XRD test results can be known using Scherrer's Equation,, $D = 0.9 \lambda / \beta \cos\theta$, where D being the crystalline size, λ is the wavelength of radiation (λ = 0.154184 nm for CuKα), θ is the Bragg angle, B is FWHM of the selected peak, and K is the material constant whose value is less than one. Commonly used values for K≈0,9 [9]. The sample microstrain size can be determined using the equation $\varepsilon = B\cos\theta / 4$ [10]. Furthermore, the milling samples were characterized using XRD and Scanning Electron Microscope (SEM) to determine the size of the grains obtained from the surface morphology of the sample. XRD used is type PANalytical X'Pert Powder Diffractometer with a wavelength CuKα of 1.54 Å. The XRD test results are identified by search & match using HighScore Plus software.

3. Results and Discussion

The characterization results using XRF obtained the manganese ores composition from west Sumatra deposit which can be seen in Table 1.

Table 1. Percentage (%) Manganese Ores Content

Element	Concentration (%)	Compound	Concentration (%)
Mn	84,139	MnO_2	78,228
Si	7,281	SiO_2	10,969
Al	5,988	Al_2O_3	8,098
Ca	0,482	*Limestone*	0,804
Cu	0,390	CuO	0,027
Ba	0,342	BaO	0,237
K	0,318	K_2O	0,258
P	0,291	P_2O_5	0,464

ISSN: 2005-4238 IJAST

The concentration of manganese element from this area is quite high yaitur 84,139%, followed by element of Si, Al and Ca with the level of% are 7,281%, 5,988% and 0,482% respectively. In XRF test also obtained data of compounds on manganese minerals such as MnO_2, SiO_2, and $AlOO_3$ with the level of% 78,228% respectively, 10,969%, and 8,098%.

Figure 1 shows the XRD results of the samples sintered with temperature variations of 26 ° C, 600 ° C, 700 ° C, 800 ° C, 900 ° C and 1000 ° C. As a result of variations in sintering temperatures there is a visible phase change from the appearance of the peak manganese oxide phase in the XRD pattern.

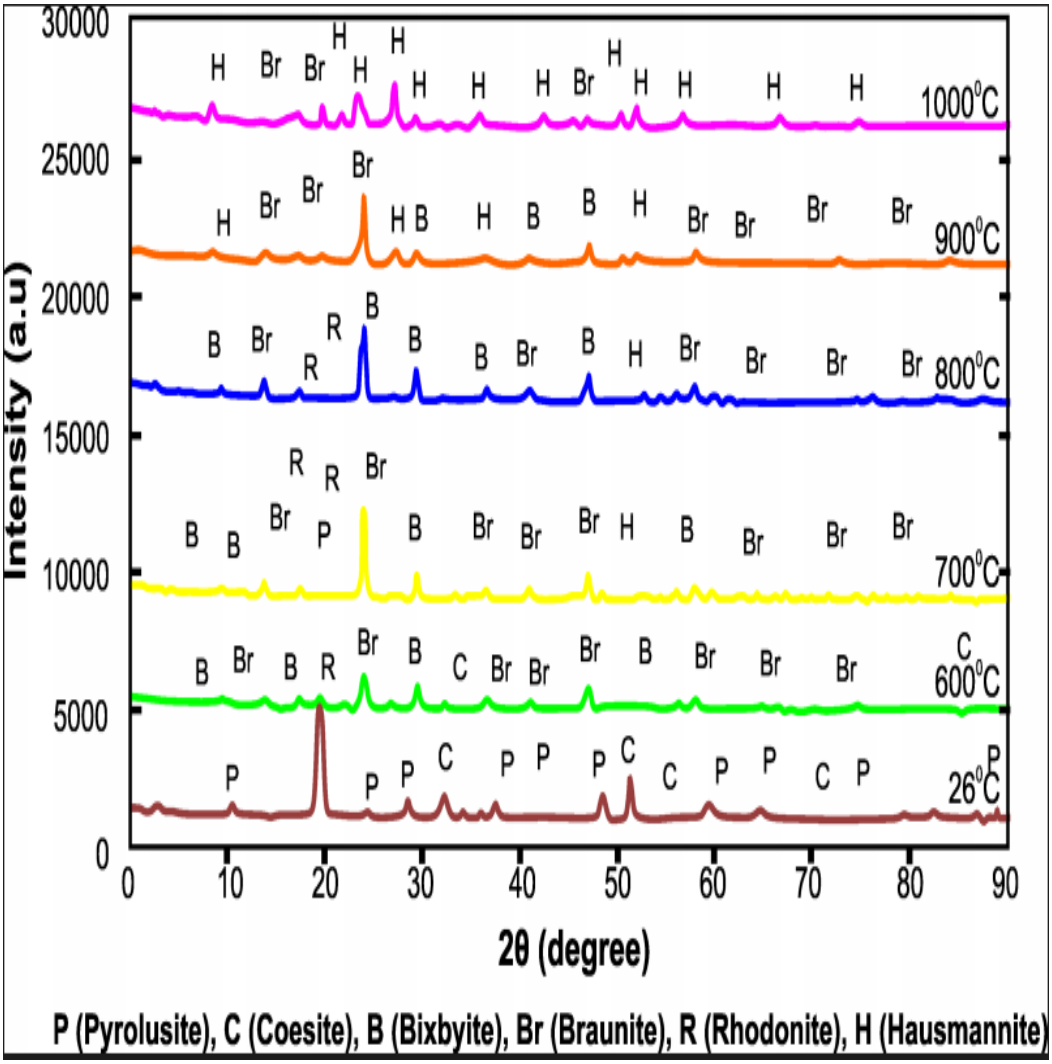

Figure 1. Manganese phase with sintering temperature variation

At room temperature found 3 types of manganese oxide phase ie pyrolusite, braunite, and coesite. In samples sintered at 600 ° C, 4 types of manganese oxide phases were found in rhodonite, bixbyite, braunite, and coesite. For samples sintered at temperatures of 700 ° C and 800 ° C there are four types of manganese oxide phases such as hausmannite, rhodonite, bixbyite, and braunite. For samples sintered at 900°C there are 3 types of manganese oxide phases such as hausmannite, bixbyite, and braunite. While samples sintered at 1000°C, only two types of manganese oxide phases are hausmannite and braunite. Figure 2 shows the XRD diffraction pattern of hausmannite after dimilling with time variations of 2 hours, 4 hours, 8 hours, and 10 hours.

ISSN: 2005-4238 IJAST

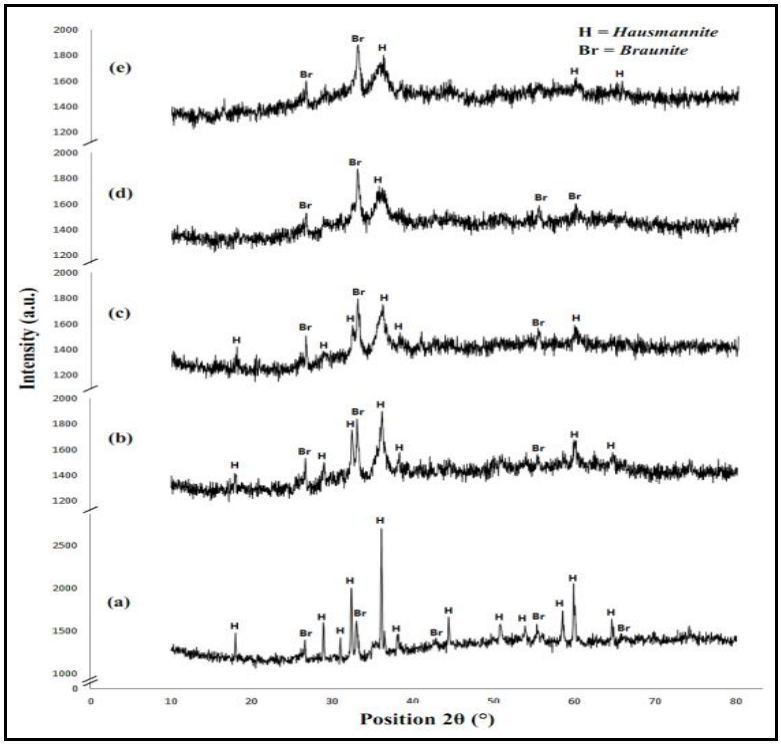

Figure 2. XRD Pattern Samples After In-Milling During: (a) 0 Hours, (b) 2 Hours, (c) 4 Hours, (d) 8 Hours, and (e) 10 Hours.

At the time of the hausmannite powder before the milling of the crystal plane is 101, 112, 200, 103, 211, 004, 220, 105, 312, 321 and 224 which corresponds to the standard value of the hausmannite tetragonal structure Mn_3O_4 ICDD No. 00-016-0154 with lattice parameters a = b = 5.7600Å, c = 9,4400Å, as well as group space I41 / amd. In this hausmannite powder there are other phases of braunite with crystal planes 204 and 224 corresponding to the standard value of the braunite tetragonal structure Mn_7O_8 (SiO_4) ICDD. 01-089-5661 with lattice parameters a = b = 9,4264Å, c = 18,6962Å, as well as space group I41 / acd.

Figure 2 shows that the peak intensity of hausmanite (36,1480) decreases and widening due to the addition of milling time up to 8 hours and then up again when the milling time is 10 hours. The decrease and widening of peaks on XRD can be caused, among others, the reduction of granules and microstrain reaction process. The sterilization of the powder of the hausmannite powder occurs because of great mechanical deformation when the milling process is performed. Where during this process there is a tremendous collision between the ball milling, hausmannite powder, and the vial wall that occurs continuously so that from the collision it will produce energy that can reduce the size of the grain.

By using the Scherrer equation we obtain a hausmanite crystalline size of 2.19 nm before dimilling. While at the time of milling 2 hours of crystalline size to be small that is 1.37 nm The crystalline size of the sample also decreases at 4 hours milling with the crystal size is 1.17 nm. However, when the milling is raised to 8 hours there is a clumping of the grain size so that the crystalline size becomes large at 1.20 nm. Then the crystalline size becomes bigger when 10 hours of milling time is 1.49 nm. The hausmannite phenomenon predominates from each sample given the milling time variation.

For milling time for 0 hours up to 4 hours the crystalline size of hausmannite decreases. This is because the hausmannite powder undergoes a collision force with steel

ISSN: 2005-4238 IJAST

balls that have strong energy so that the hausmannite powder becomes eroded again and becomes small. However, at the time of milling for 8 hours and 10 hours the crystalline size of hausmannite becomes increased, this occurs because the sample has agglomeration due to increased grain size at the time of the milling process. Giving the old milling time will cause the vial temperature increases due to rotational speed rotation of the ball that occurs continuously then the collision energy generated greater so that the resulting temperature is also higher. As the temperature rises inside the vials there is an increase in thermal energy that causes crystal growth, so the nucleus grows by attracting other atoms or diffusing from other unchained nuclei to fill the empty space on the lattice to be formed. Mechanical activation provided with milling using HEM-E3D results in faster diffusion in regions where the atomic arrangement is more random, as the energy becomes larger and the movement of atoms also becomes easier. Thus, the growing thermal energy of crystal growth continues until the final transformation of the crystal occurs. The graph of crystal size change to this milling time variation can be seen in Figure 3.

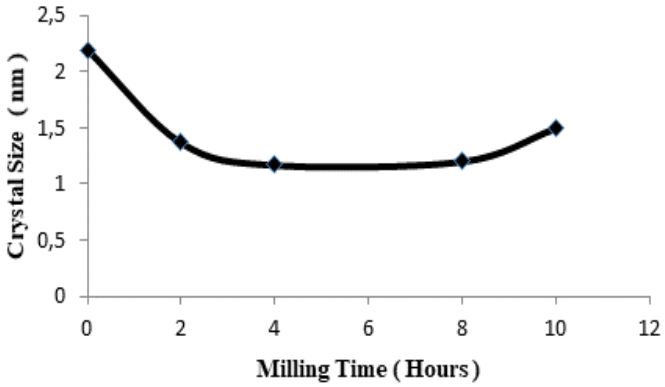

Figure 3. The Relation between Milling Time on Crystal size Changes

To find out the surface structure and particle size of hausmanite is used SEM [11]. Figure 4 is a morphology of hausmannite powder before being milled with 10,000X and 40.000X magnification.

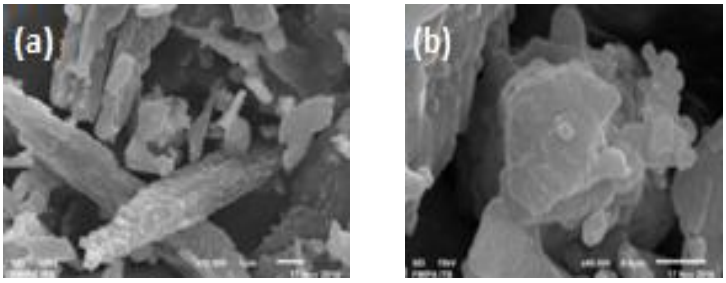

Figure 4. The Hausmannite SEM test results before being milled with magnification (a) 10.000X, (b) 40.000X

Hausmanite has an irregularly shaped morphology of particles and random particle distribution from the smallest size to the largest size. Based on the morphology of the hausmannite powder before the milling was obtained the size of the grain is 1.32 μm. Figure 5 is the surface morphology of the hausmannite powder after milling for 2 hours, 4 hours, 8 hours, and 10 hours.

ISSN: 2005-4238 IJAST

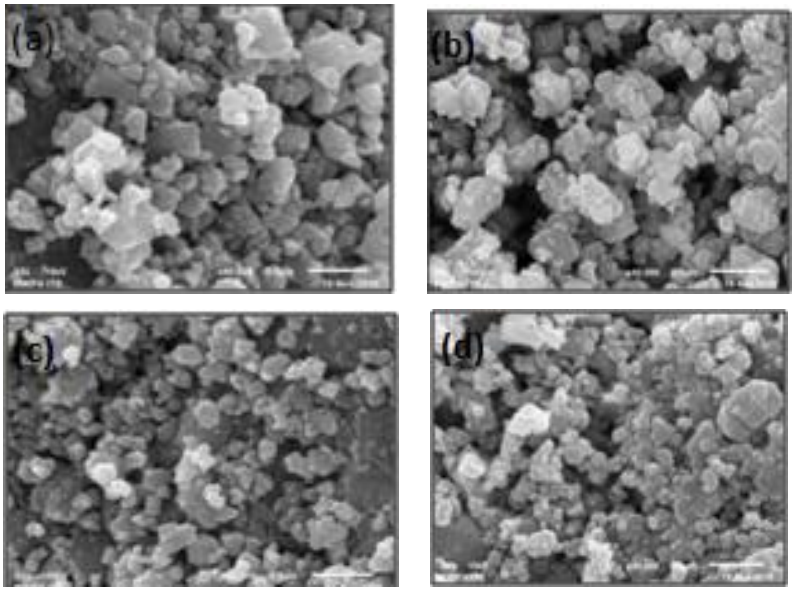

Figure 5. Differences of Sample Morphology For Each Variation of Milling Time with Magnification 40,000X (a) 2 Hours, (b) 4 Hours, (c) 8 Hours, and (d) 10 Hours.

At the time of 2-hour milling (Figure 5 (a)), the particle shape was smaller than the sample morphology before it was milling and the size distribution was uneven. The average grain size is 299.50 nm. This particle size reduction occurs also when samples are milled for 4 hours (Figure 5 (b)) and the size distribution is also uneven. The average grain size is 193.50 nm This particle size decreases when it is milling for 8 hours (Figure 5 (c)). At the time of this 8 hour milling, sample particle size distribution has been formed almost evenly and homogeneous. The particle size produced is 90.50 nm. However, when samples are milled for 10 hours (Figure 5 (d)) there is agglomeration of the particles causing the size of the particle to re-enlarge with the grain size being 182.00 nm.

The milling time may affect the size of the crystal grains in the sample. This is because during the milling process, the powder particles will experience the process of repeated destruction. When the milling balls collide with each other then the milling powder is between the collisions of the balls causing the deformed powder and the powder to be destroyed, causing the grain size of the powder to become small and so on until it reaches the nano size. It can also cause agglomeration of sample granules so that the grain size increases again. Figure 6 shows a change in grain size of hausmanite to a variation of mausmannite milling time.

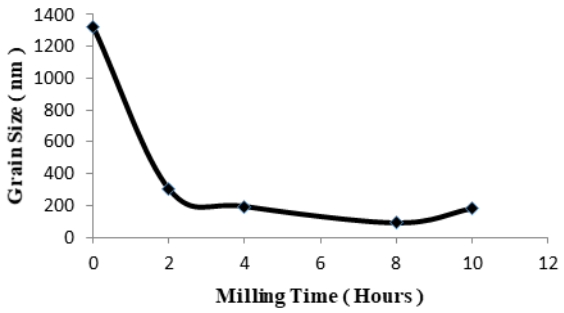

Figure 6. Relationship between Milling Time on Grain Size Change

ISSN: 2005-4238 IJAST

Hausmannite morphological differences are also seen in each variation of milling time. This is because the granules are clumping between the grains with each other and the grain shape is not evenly distributed. The magnitude of the grain size in one of the milling results is due to the atom diffusion process and the particle agglomeration. This process of atomic diffusion occurs due to the length of time the milling is given. The longer the milling time will increase the temperature on the collision of the milling balls. Increased temperatures in the milling is what causes the diffusion process between the particles more quickly occur because of the greater the energy so that the movement of atoms more easily and make the size of grains enlarged.

Agglomeration process that occurs can also be caused by several things, namely the contamination of sample powders with crushing ball material and vials. Despite its extremely high hardness, the stainless steel on the crushing bulb and vial will still contaminate the milled sample powder. High milling rates and long grinding times cause contamination of crush-and-vial binder-forming materials to be virtually unavoidable [12-13]. Grain agglomeration of hausmannite nanoparticles is shown in Figure 7.

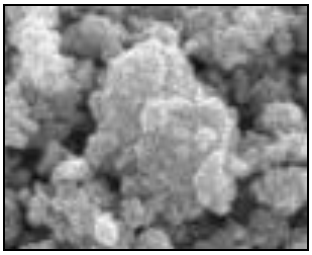

Figure 7. Agglomeration Occurring On Hausmannite Nanoparticles

The agglomeration occurring in the hausmannite nanoparticles causes the size of the grains to become larger than the surrounding grain size. This indicates that the length of time the milling is given does not necessarily decrease the size of the grains of the hausmannite nanoparticles.

4. Summary

The hausmannite nanoparticles (Mn_3O_4) have been synthesized using the High-Energy Milling method. Synthesis is done by varying the temperature and time of milling. The synthesis results show that the hausmanite phase occurs at 700^0C sintering temperature. The hausmannite nanoparticles with a homogeneous distribution formed at 8 hours of milling time. The grain size of the resulting hausmannite nanoparticles is 90.50 nm. An increase in milling time above 8 hours causes the hausmannite nanoparticles to become clumped and their grain size enlarged.

Acknowlegment

The authors thank to RISTEK DIKTI for financial support through Hibah MP3EI 2017 for this work.

References

[1] Nichol, Ian. 1962. *A Study of Some Manganese Minerals*. Durham theses, Durham University.
[2] Baba, A. A. *et al*. 2014. "Hydrometallurgical Processing of Manganese Ores: A Review." *Journal of Minerals and Materials Characterization and Engineering*, 2, 230-247.

ISSN: 2005-4238 IJAST

[3] Vazquez-Olmos, America. *et al*. 2005. "Structural and Magnetic Study of Mn_3O_4 Nanoparticles." *Rev.Adv.Mater.Sci*. 10 (2005) 362-366. y.
[4] Tavangarian. R, Emadi. R. 2009. *Mechanical Activation Assisted Synthesis Of Pure Nanocrystalline Forsterite Powder*. Department of Materials Engineering, Isfahan University of Technology (IUT), Isfahan 84156-83111, Iran. pp. 648-652
[5] Jiang, Hao. *et al*. 2010. "Hydrothermal Synthesis of Novel Mn_3O_4 Nano-Octahedrons with Enhanced Supercapacitors Performances." *Nanoscale*, 2, 2195-2198.
[6] Herrera-Miranda, D. *et al*. 2012. "High Surface Area Nanocrystalline Hausmannite Synthesized by a solvent-free route." *Materials Research Bulletin* 47 (2012) 2369-2374
[7] Lakshmi, S.Vijaya., Pauline, S., Vinosel, V.Maria. 2014. "Microstructural Characteriztion of Trimanganese Tetra Oxide (Mn3O4) Nanoparticle by Solvothermal Method and Its Dielectric Studies." *International Journal Of Engineering Sciences & Research Technology*. ISSN: 2277-9655.
[8] Suryanarayana, C. and Norton, M. Grant. 1998. *X-Ray Diffraction A Practical Approach*. Springer Science+Business Media New York.
[9] Shrividhya, T. *et al*. 2013. "Synthesis and Study on Structural, Morphological, and Magnetic Properties of Nanocrystalline Manganese Oxide." *Internasional Journal of Science and Engineering Applications Special Issue* NCRTAM ISSN-2319-7560.
[10] Usha, K. *et al*. 2011. "Structure, Morphology and Electrical Properties of Mn_3O_4 nanocrystals." *Arch. Phy. Res.*, 2(1) : 75-80 ISSN 0976-0970.
[11] Calka. A and Nikolov J. I. 1995. "The Dynamics of Magneto-Ball Milling and its Effects on Phase Transformations During Mechanical Alloying." *Materials Science Forum* vol. 179–181, pp. 333–338.
[12] Ratnawulan, Fauzi, A., & Zahara, Y. (2018). Influence of high energy milling time on nano-quartz structure from West Sumatera. *Journal of Physics: Conference Series*, *1040*, 012048. doi: 10.1088/1742-6596/1040/1/012048
[13] Sarimai, Ratnawulan, Yulkifli, & Fauzi, A. (2019). Fabrication of superhydrophobic CuO/polystyrene nanocomposite coating with variation concentration. *Journal of Physics: Conference Series, 1185*, 012014. doi: 10.1088/1742-6596/1185/1/012014

ISSN: 2005-4238 IJAST